Ultrasonic attenuation and dislocation damping in helium crystals

Fujio Tsuruoka and Yosio Hiki
Tokyo Institute of Technology, Oh-okayama, Meguro-ku, Tokyo 152, Japan
(Received 14 May 1979)

Measurements of the attenuation of pulsed longitudinal sound at frequencies of 5, 15, 25, 35, and 45 MHz have been made in hcp ^{4}He crystals grown under constant pressure of 32.5 and 60.0 atm at molar volumes of 20.5 and 19.2 cm^3/mole. The specimens used for the measurements were considered to be single crystals. The attenuation versus frequency dependence measured for a number of crystals always revealed a broad peak. The height of the peak was dependent on the crystallographic orientation of the specimens. When the temperature was suddenly changed, the peak gradually shifted to a new location. The frequency dependence of the attenuation was measured at various temperatures between 1.3 and 2.3 K, and the height and location of the peak were found to be dependent on temperature. It was also found that the attenuation increased markedly when the strain amplitude of ultrasound was increased above a certain level. By the analysis of these experimental results the following conclusions have been obtained: The main origin of the attenuation is the overdamped resonance of crystal dislocations; the slip plane of the dislocations is the basal plane; the dominant pinning points are jogs existing on the dislocations in thermal equilibrium; the damping of dislocation motion originates from the energy loss due to three-phonon processes between thermal phonons and quasilocal phonons around dislocations. The argument was essentially classical, and the quantum character of dislocations was thus far not taken into consideration.

I. INTRODUCTION

Helium is unique in that it does not freeze under its saturated vapor pressure even at the lowest temperature, and solidification can only occur when a considerable pressure is applied. This is a consequence of the quantum-mechanical large-amplitude zero-point motion of atoms, and thus solid helium is labeled a quantum solid. Under the stimulus of this point, a great deal of theoretical and experimental investigations have been made concerning solid helium.[1–4] The acoustic method is powerful in investigating the properties of the crystal lattice. There have been many experimental studies on sound velocities in various phases of ^{4}He and ^{3}He crystals. In this respect, solid helium is distinctive in its small sound velocities, and this is due to the weak interactions between atoms in the crystal. It is regrettable, however, that there has been no extensive study of ultrasonic attenuation in this material, since attenuation measurements are able to reveal much about the properties of crystals.

The present authors have started the attenuation experiment in hcp ^{4}He crystals with interest as to whether or not the characteristic features of quantum solid would be detected.[5] Afterward, our experimental results were found to be reasonably explained by the mechanism of dislocation damping, namely, the acoustic loss arising from the vibration of dislocations in crystals.[6,7] The problem of lattice defects in quantum solids is also a very interesting subject.[4] There are many studies on the point defects in solid helium, while those on crystal dislocations in the material are still very few. We found that attenuation measurement was well adapted to study the properties and behavior of dislocations in solid helium. A preliminary summary of our work has been issued[8] in which a semiquantitative interpretation of our experiments has been given. We present in this article our experimental results in more complete form, and the analysis of the results in a more thorough and consistent manner.

II. EXPERIMENTAL METHOD

Crystals of hcp ^{4}He were prepared by cooling normal liquid helium in a sample cell. They were grown under constant pressure of 32.5 and 60.0 atm at molar volumes of 20.5 and 19.2 cm^3/mole. A pulse reflection method[9] was used in the attenuation measurements with longitudinal sound at frequencies of 5, 15, 25, 35, and 45 MHz. The measurements on the crystals were made at temperatures between 1.3 and 2.3 K.

A. Sample cell and cryogenics

The construction of our sample cell is illustrated in Fig. 1. The main body is made of a copper block with a cylindrical cavity and a couple of stainless steel flanges to support a quartz transducer and a reflecting

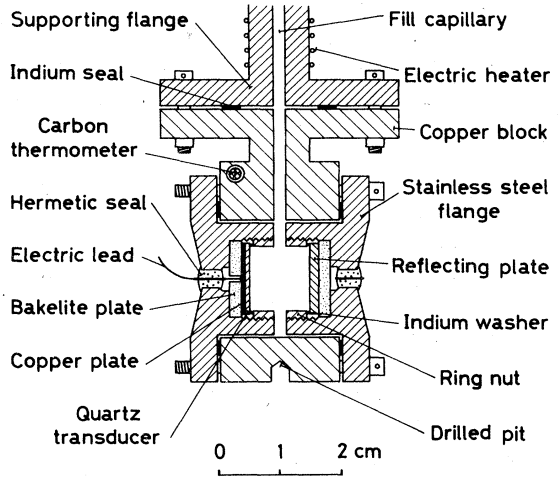

FIG. 1. Cross-sectional view of sample cell.

plate. Six stainless-steel screws and indium wire seals are used to assemble these parts. The assembly is attached to a supporting flange connected to the capillary tube for supplying sample helium. The cell is dipped in liquid helium in a glass Dewar. On the outer bottom of the cell wall, a pit is drilled so as to produce a cold spot on the inner bottom of the cell. An electric current in the heater wound around the fill capillary produces an upwards temperature gradient. These circumstances are favorable in growing a single crystal in the cell. The heater is also used to prevent the capillary from blocking before the crystal growth is completed. The cell has a hole in which a carbon thermometer is inserted with Apiezon grease.

The sample cell is designed to be used either for the pulse reflection or the pulse transmission method. In the present experiment, the reflection method was used. A 5-MHz X-cut quartz transducer, gold plated on both faces, and an optically flat fused-quartz reflecting plate are set inside the cell. Care was taken in the method to support both of them, this being important in order to obtain intense and stable pulse echoes, especially at higher frequencies. Indium wire washers and stainless-steel ring nuts were used for that purpose. Bakelite back plates are used for obtaining intense pulse echoes and also for electric insulation. The hermetic seals can safely be used repeatedly at low temperatures and under pressures up to 70 atm. The electric lead from the transducer is connected to a coaxial cable made of stainless-steel wire and tube. Parallel setting of the transducer and the reflecting plate is achieved as follows. The end faces of the copper block are polished, and the stainless-steel flanges are fixed to the copper block. Then the cell is filled with distilled water, and the ultrasonic echo patterns are observed. This procedure is repeated until a regular exponential pattern having the maximum number of ultrasonic pulse echoes, about thirty, is obtained. The parallelism is estimated to be better than 10^{-5} radian, as described later.

The temperature of the cell is lowered by pumping the liquid helium in the Dewar, and is measured by mercury and oil manometers within an error of 3 mK at 1.7 K, and is also monitored by the carbon thermometer connected to a potentiometer and a recorder. The temperature is controlled manually by adjusting the pumping speed, and can be held constant within 1 mK. The pressure inside the cell is measured with a Heise-Bourdon gauge with an accuracy of 0.05 atm.

B. Crystal growth

After being passed through two charcoal traps cooled with liquid nitrogen, pressurized commerical grade (99.995%) helium gas is introduced into the cell and then condensed. At first the round-trip time of ultrasonic pulses in liquid helium is measured at a temperature T_A (=2.20 K for the applied pressure $P=32.5$ atm and 2.70 K for $P=60.0$ atm). The acoustic path length between the transducer and the reflecting plate is determined using the existing sound velocity data of liquid helium.[10] Then the temperature of the cell is gradually reduced at the rate of 1–3 mK/min. The liquid helium inside the cell is not solidified at the temperature on the existing melting curve T_B (=1.86 and 2.52 K for $P=32.5$ and 60.0 atm), but is always supercooled to a temperature T_C ($\approx$1.76 and 2.30 K for $P=32.5$ and 60.0 atm). Solidification is detected by observing an anomaly in the temperature-recording chart or by observing a change in the ultrasonic echo patterns. Then the inlet tube is blocked by cutting off the electric current in the heater. Note that the volume of the specimen, and not the pressure, is kept constant after the blocking. The temperature of the crystal is slowly reduced to T_D (=1.70 and 2.25 K for $P=32.5$ and 60.0 atm) at the rate of 1–2 mK/min. After keeping the temperature constant at T_D for 30 min, attenuation and velocity measurements are started on the crystal.

The molar volume of the crystal is determined by the existing melting curve,[11] after regarding the measured pressure at T_C as the melting pressure. The crystallographic orientation of the grown crystal is determined from the sound velocity value. The velocity of sound in hcp crystals depends only on the angle θ between the direction of sound propagation and the crystallographic c axis.[9] The elastic constants of hcp ^{4}He crystal have been determined as functions of molar volume by several investigators.[12–15] Thus the longitudinal sound velocities can be calculated as functions of the angle θ with the molar volume V_m as a parameter. For example, in crystals with $V_m=20.5$

cm^3/mole, the velocity is 585 and 509 m/sec at $\theta = 0°$ and 90°, and has a minimum value of 494 m/sec at 58.5°. The velocity varies slowly with θ at $\theta = 0°$ and 90°, and the variation is most rapid at $\theta \approx 30°$. The value of θ is double valued in the range $44° < \theta < 90°$, except at $\theta \approx 59°$. The errors in the orientation angle determined from the velocity value are 3%–10%, being dependent on the orientation.

There are three kinds of procedure to grow helium crystals: growth under constant pressure, at constant volume, and at constant temperature. The first method has been considered to be the best in growing good single crystals, which was verified by an x-ray method[14] and by an optical birefringence method.[16] In the present experiment, about two hundred crystals have been grown and about one fourth of them were regarded as good single crystals after inspecting their ultrasonic pulse echoes. Crystals with a small number of echoes, with irregular patterns of echoes (not exponentially decayed or not equally spaced), and with unreasonable values of sound velocities were considered to be polycrystals or inhomogeneous crystals, and were not used in the attenuation measurements.

C. Acoustic measurements

The electronic apparatus used were an ultrasonic generator and receiver (Matec model 6000 + 750 or 760) and a synchronizer and exponential generator (model 1204*A*). Also, an attenuator and impedance matching circuits were used in the usual manner. The attenuation is measured on an oscilloscope by adjusting the calibrated exponential curve to coincide with the envelope of the pulse echoes, and the sound velocity is determined from the flight time measured by a calibrated delayed time marker, using the acoustic path length already determined. The minimum readings in the attenuation and the time values are 0.005 dB/μsec and 0.2 μsec, respectively. The numbers of echoes observed in usual helium crystal specimens are 10–20 at 5 MHz and are reduced to 2–3 at 45 MHz.

Possible sources of error in the attenuation measurement will be considered in the following.

(a) Transmission loss. The reflection coefficient for a plane wave incident normally on a boundary between medium 1 and medium 2 is

$$R = \left(\frac{\rho_1 c_1 - \rho_2 c_2}{\rho_1 c_1 + \rho_2 c_2} \right)^2 , \tag{1}$$

where ρ_i and c_i are the density and the sound velocity in the ith medium. For solid helium and quartz, $\rho_1 = 0.2$ g/cm^3, $c_1 = 5 \times 10^4$ cm/sec and $\rho_2 = 2.2$ g/cm^3, $c_2 = 6 \times 10^5$ cm/sec. Therefore, in the present case R is almost 100%, and the loss caused from the transmission of waves out of the end faces of the specimen is negligible.

(b) Diffraction loss. When an ultrasonic wave with wavelength λ excited by a circular transducer with radius a propagates distances farther than $x_0 = a^2/2\lambda$, spreading of the beams occurs and diffraction loss arises. For the case of 5 MHz sound in helium crystals and for $a = 0.6$ cm, this distance becomes $x_0 = 18$ cm, which corresponds to the distance for ten pulse echoes. We used more than ten echoes for the attenuation measurements, so the diffraction loss should be considered. The apparent attenuation caused from the loss is roughly estimated as[9]

$$\Delta\alpha = 1/(a^2/\lambda) = 2.8 \times 10^{-2} \text{ dB/cm}$$
$$= 1.4 \times 10^{-3} \text{ dB/}\mu\text{sec} . \tag{2}$$

This is 7% of the minimum value of the attenuation measured in our helium crystals, 0.02 dB/μsec. The loss becomes even smaller for the case of sound with higher frequencies.

(c) Effect of nonparallelism. When the transducer and the reflecting plate are not accurately parallel to each other, an apparent attenuation is observed, the magnitude of which is estimated to be[9]

$$\Delta\alpha = \frac{8.686\pi^2 f^2 a^2 \delta^2 n}{cL} \text{ dB/sec} , \tag{3}$$

when the nth echo is observed. Here f and c are the sound frequency and velocity, L is the acoustic path length, and δ is the angle of inclination. From this formula, the angle δ has been evaluated by measuring the attenuation in distilled water filled in the sample cell and by comparing the value with those determined accurately by other authors.[17] The result was $\delta \leq 10^{-5}$ radian. Then the value $\Delta\alpha$ is estimated to be smaller than 10^{-3} dB/μsec for the case of attenuation measurement at 25 MHz in helium crystals. The parallel setting seems to be not disturbed when the sample cell is cooled slowly to low temperatures, since the attenuation shows a reasonable value for liquid helium condensed in the cell.

(d) Measurement error. In practice, the largest error in the attenuation measurement may arise from the fitting of the exponential curve to the echo pattern, especially when the number of echoes is not so large. The errors were estimated from repeated fitting of the curve, and they were typically 3% at 5 MHz and 20% at 45 MHz.

III. RESULTS AND ANALYSIS

There are two important external variables in acoustic loss measurements: the frequency and the amplitude of the vibration. Temperature is another variable, as in usual solid-state experiments. Crystallographic orientations and, in the case of solid heli-

TABLE I. Constant values of hcp ^{4}He.

Melting pressure P_M (atm)		32.5	60.0
Melting temperature T_M (K)[a]		1.86	2.52
Molar volume V_m (cm^3/mole)[a]		20.5	19.2
Density ρ (g/cm^3)[a]		0.195	0.208
Lattice parameter a (10^{-8} cm)[b]		3.64	3.56
Burgers vector b (10^{-8} cm)			
Elastic constants c_{ij} (10^8 dyn/cm^2)[c]	c_{11}	5.05	7.67
	c_{12}	2.69	4.24
	c_{13}	1.35	1.97
	c_{33}	6.68	9.85
	c_{44}	1.35	1.97
Shear modulus G (10^8 dyn/cm^2)[d]		1.47	2.16
Poisson's ratio ν[d]		0.294	0.298
Debye temperature Θ_D (K)[e]		25	28

[a]Reference 11.
[b]Calculated from the data by V. J. Minkiewicz, T. A. Kitchens, F. P. Lipschultz, R. Nathans, and G. Shirane, Phys. Rev. 174 267 (1968).
[c]Deduced from the data in Refs. 12–15.
[d]Averaged value by the method of Voigt and Reuss. See O. L. Anderson, in *Physical Acoustics*, edited by W. P. Mason (Academic, New York, 1965), Vol. IIIB, p. 43.
[e]Estimated from the data by G. Ahlers, Phys. Rev. A 2, 1505 (1970).

um, molar volumes of crystals are also important parameters. We have conducted experiments which were intended to show the dependences of ultrasonic attenuation on these variables and parameters. The results are analyzed consistently on the basis of the dislocation damping mechanism. Other possible origins of the sound attenuation will be discussed later.

Values of various physical constants of helium crystals used in the present analysis are collected in Table I as a reference.

A. Frequency dependence

In the following, the acoustic loss is represented by the decrement or the internal friction Δ, defined as the energy loss per cycle of vibration divided by twice the vibrational energy. In the case of small decrement, it is related to the ultrasonic attenuation as

$$\Delta = \alpha c / f \ , \tag{4}$$

where α is the attenuation coefficient in nepers/cm, c is the sound velocity in cm/sec, and f is the frequency in Hz.

The experimental results on the frequency dependence of decrement are illustrated in Fig. 2. Specimens are distinguished by their molar volume V_m and their orientation angle θ. The error bars indicate the uncertainty in the measured values estimated as discussed before. The Δ-vs-f plot always reveals a broad peak, and the height and location of the peak maximum are different in different crystals and also are dependent on temperature. These situations are often observed in ordinary crystals, and are well explained by the theory of the overdamped resonance of vibrating crystal dislocations.[18,19] We will adopt the theory to analyze our experimental results.

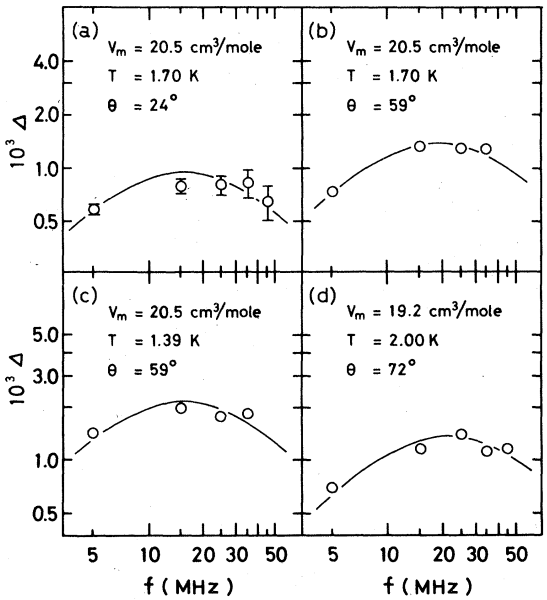

FIG. 2. Frequency dependence of decrement. The curves represent the results of parameter fit.

B. Resonance loss

In the theory of Granato and Lücke,[18] dislocation lines fixed by discrete pinning points and forced into vibration by an acoustic wave are considered. The loop of dislocation is regarded as a string of length L, the pinning length, vibrating in a viscous medium, and the equation of motion is

$$A\frac{\partial^2 u}{\partial t^2}+B\frac{\partial u}{\partial t}-C\frac{\partial^2 u}{\partial y^2}=b\sigma \ , \tag{5}$$

where u is the displacement of dislocation, y is the coordinate along dislocation, A $(=\pi\rho b^2)$ is the effective mass of dislocation, B is the damping constant, C $[=2Gb^2/\pi(1-\nu)]$ is the line tension, b is the Burgers vector, σ is the stress produced by the acoustic wave, and ρ, G, and ν are the density, shear modulus, and Poisson's ratio of the material. The acoustic wave impinging on the dislocation loses its energy through the damping term, and the loss is dependent on the sound frequency. Sharp resonance absorption occurs at the angular frequency $\omega_0=(\pi/L)(C/A)^{1/2}$ when $D=\omega_0 A/B$ is large. When the value of D is small, namely, for the case of large damping, the decrement versus frequency shows a broad peak and the peak maximum is located at a frequency lower than ω_0. In this case of overdamped resonance, the decrement can be expressed as

$$\Delta_r=\frac{\Delta_0\omega\tau}{1+\omega^2\tau^2};\quad \Delta_0=8n\,\Omega\,Gb^2\Lambda L^2/\pi^3 C \ , \qquad \tau=n'BL^2/\pi^2 C \ . \tag{6}$$

Here Λ is the dislocation density, Ω is the orientation factor for taking into account the fact that a dislocation can move in a definite direction on a definite slip plane, and $n=n'=1$ or $n=4.4$, $n'=11.9$ for the δ function or the exponential distribution of the pinning points on the dislocations. The decrement has a maximum value of $\Delta_m=\frac{1}{2}\Delta_0$ at the frequency $f_m=1/2\pi\tau$.

The above-stated formulas were used to analyze the present experiment on frequency-dependent decrement. The values of two quantities Δ_m and f_m were determined by a least-squares fit of the data to the theoretical formulas. The curves in Fig. 2 represent the fitted ones, and the fitting is reasonably good.

C. Orientation dependence

The frequency dependence of decrement was measured for a number of crystals at $T=1.70$ and 2.25 K for $V_m=20.5$ and 19.2 cm^3/mole specimens, and the Δ_m and f_m were determined. In Fig. 3(a) and 3(b), the two quantities $f_m\Delta_m$ and $f_m^{-1/2}$ are plotted against the orientation angle θ of the crystal. Data for specimens which are double valued in orientations are shown by small black circles and large circles. The quantity $f_m\Delta_m$ is strongly orientation dependent, while the quantity $f_m^{-1/2}$ is not.

From the theory of overdamped resonance of dislocations, the two quantities are represented as

$$f_m\Delta_m=(2nGb^2/\pi^2 n')(\Lambda/B)\,\Omega \ , \qquad f_m^{-1/2}=(2n'/\pi C)\sqrt{B}L \ . \tag{7}$$

A general method for calculating the orientation factor Ω has been developed for the traveling-wave (MHz measurement) and the standing-wave (kHz measurement) cases.[20] We assume that the slip plane in the hcp ^{4}He is the basal plane, and calculate the Ω for a traveling longitudinal wave (see Appendix A). The orientation factor is zero for $\theta=0°$ and 90°, since sound waves propagating normal or perpendicular to the slip plane do not produce a shear stress component on the dislocation. A constant multiple of Ω was fitted to the experimental values of $f_m\Delta_m$, and the curve in Fig. 3(a) represents the result, showing a fairly good fit. The scatter in the data may be mainly due to the differences of dislocation density in different crystals. In this plot we use the quantity $f_m\Delta_m$ and not Δ_m, because the latter contains both the dislocation density and pinning length, and the scatter is magnified when it is adopted. It is not-

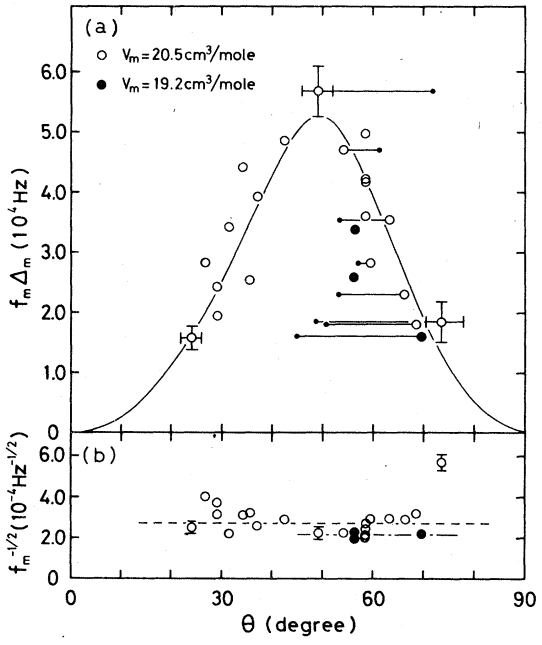

FIG. 3. (a) Orientation dependence of $f_m\Delta_m$. The curve represents the result of fit. (b) Values of $f_m^{-1/2}$. The broken lines represent the average values.

ed here that the orientations of crystals which are double valued can be uniquely determined after observing the values of $f_m\Delta_m$. The orientation angles corresponding to the data points represented in the figure by large circles are considered to be determined. The value of $f_m\Delta_m$ seems to be very small at $\theta=0°$ and $90°$, which shows that the main origin of the acoustic loss is due to dislocation damping in the present case.

The orientation independence of $f_m^{-1/2}$ shown in Fig. 3(b) is as expected from the theory. The scatter in the data may be due to the differences of pinning length. However, the scatter is not so large, about 20% above and below the average. The average values of $f_m^{-1/2}$, which are shown by the broken lines in the figure, are somewhat different for crystals with different molar volumes. This may be caused by the differences in values of C and B, and in average values of L for the two kinds of crystals.

It can be concluded here, from the frequency dependence and the orientation dependence experiments, that (i) the overdamped resonance of dislocations is the main origin of the attenuation, (ii) the slip plane of dislocations is the basal plane, and (iii) the specimens used are considered to be single crystals.

D. Pinning points

To develop the present study further, consideration of pinning points on dislocation lines is desired. Impurity atoms are able to pin down a dislocation, and the concentration of impurities on a dislocation is

$$c = c_0 \exp(E_i/k_B T) \ , \tag{8}$$

where c_0 is the impurity concentration in the crystal, k_B is the Boltzmann constant, and E_i is the interaction energy between the impurity and the dislocation. The elastic interaction energy can be calculated as[21]

$$E_i = [G(1+\nu)/3\pi(1-\nu)]4\pi b^3\epsilon \ ,$$

where ϵ is the misfit parameter for the solute and the solvent atoms. In the case of ^{4}He crystals, the only possible impurities are ^{3}He atoms. Their concentration c_0 is usually considered to be 1 ppm or less, and ϵ can be calculated from the molar volumes of the ^{3}He and ^{4}He crystals with the same melting pressure. It turns out that $\epsilon=\frac{1}{45}$ and $E_i=3.8\times10^{-16}$ erg for $V_m=20.5$ cm^3/mole, and then $c=5.0\times10^{-6}$ for $c_0=1$ ppm and $T=1.70$ K. The value of c is very small and therefore ^{3}He impurities are not effective pinning points. Vacancies are other point defects which interact with dislocations, but they are extremely movable in solid ^{4}He and cannot be stable pinning points. Kinks on dislocations are easy to move since they are on the slip plane, and are also excluded from consideration. Crystal dislocations form a three-dimensional network and their nodal points can be very stable pinning points.

Other possible pinning agencies considered were jogs on dislocations. A number of jogs can exist on dislocation lines in thermal equilibrium,[22] and the motion of jogs should be hindered because of the high Peierls stress, so that the jogs are able to pin down dislocations.[23] In a hcp ^{4}He crystal as shown in Fig. 4, we consider the $\langle 10\bar{1}0\rangle$ edge dislocation with $\frac{1}{3}\langle 1\bar{2}10\rangle$ Burgers vector, and further consider the $\langle 10\bar{1}\bar{1}\rangle$ jogs which are shortest in length. Jogs with short length and small self-energy will be most favored to form. The increase of the configurational entropy due to jog formation is shown to be $k_B \ln[2^{n/2}N!/n!(N-n)!]$, where N and n are the numbers of atoms and jogs on the unit length of dislocation. The number of jogs in thermal equilibrium can be calculated from the condition of minimum free-energy. The vibrational entropy is omitted, since it is small compared with the configurational entropy. The pinning length $L(=1/n)$ is then given as

$$L = \sqrt{6}b \exp(E_{\text{jog}}/k_B T) \ . \tag{9}$$

The self-energy of a jog E_{jog} is shown to be[24]

$$E_{\text{jog}} = b^2 b' G/4\pi(1-\nu) \ , \tag{10}$$

and here b' is the length of the jog. In crystals with $V_m=20.5$ cm^3/mole, $b'\approx b$ and the jog energy is $E_{\text{jog}}=8.0\times10^{-16}$ erg. Then the pinning length is $L=2.7\times10^{-6}$ cm at $T=1.70$ K. The value of L is smaller than the network length of dislocations L_N which is usually considered to be 10^{-5}–10^{-4} cm (see Fig. 4). The concentration of jogs on dislocation $c=n/N$ is about 10^{-2}, which is very large. This large concentration or small pinning length originates from the small value of G and therefore of E_{jog} in helium crystals. Thus it is considered that the jogs are effective in pinning the dislocations. It should be remembered that the values of $f_m^{-1/2}$ in Fig. 3(b), which is

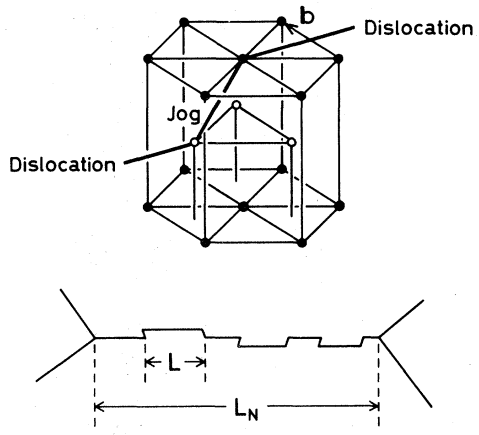

FIG. 4. Jog-pinning model

proportional to the pinning length L, are not so different among crystals with the same molar volume. This fact is favorable to the present idea of dislocation pinning by thermal equilibrium jogs.

It is noted here that the pinning jogs are actually distributed randomly on the dislocation lines. The length L in Eq. (9) represents the mean pinning length. As the case of the impurity pinning,[18] the number of dislocation loops with lengths between l and $l+dl$ is

$$N(l)\,dl = (\Delta/L^2)\exp(-l/L)\,dl \quad , \tag{11}$$

where Λ is the dislocation density in the crystal.

E. Time dependence

The following experiment has been made to obtain information concerning the pinning points. After the temperature of a crystal was held constant for a sufficiently long time, it was suddenly changed at a rate of several mK/min to another temperature and then kept constant. The frequency dependence of the attenuation was then measured at adequate time intervals. The quantity $f_m^{-1/2}$ determined from the attenuation-versus-frequency curve is illustrated in Fig. 5 as a function of elasped time for the case of sudden decrease Figs. 5(a) and 5(b) and sudden increase Fig. 5(c) of temperature. The value of $f_m^{-1/2}$, which is proportional to the pinning length L, gradually increases or decreases to a new equilibrium value. This result is favorable to the jog-pinning model, since the equilibrium value of L is smaller at high temperatures, as can be seen from Eq. (9). In the case of impurity pinning, the behavior should be in the opposite direction [see Eq. (8)]. It is also difficult to imagine that the network length of dislocations changes systematically when temperature is changed. The predominance of jog pinning thus appears to be probable in helium crystals in the present case.

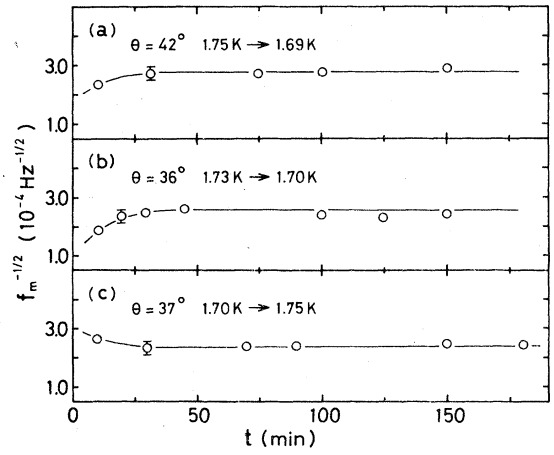

FIG. 5. Changes of $f_m^{-1/2}$ with time after temperature is suddenly decreased (a), (b) and increased (c).

F. Amplitude dependence

It is often observed that the decrement in crystals is enhanced markedly when the amplitude of vibration becomes sufficiently large, and this phenomenon can be successfully explained by considering the hysteresis loss arising from the depinning of dislocations from the pinning points.[18] From the experiment on the amplitude dependence of decrement, one can obtain much knowledge about the pinning points. Such measurements are usually made at kHz range frequencies. The MHz sound waves can be used for soft materials,[25] since the amplitude of ultrasonic waves is large in them.

The attenuation of 5 MHz sound has been measured at 1.70 K in helium crystals with $V_m = 20.5$ cm^3/mole, and the amplitude of the wave was varied by changing the voltage applied to the ultrasonic transducer. Results for two different crystals are shown in Fig. 6, where decrement Δ is shown as a function of S, which is the relative value of the applied transducer voltage read by an attenuator in the electric circuit. Large amplitude dependence can be seen, and the Δ-vs-S is reversible, namely, Δ is the same when S is increased and again decreased. No meaningful temperature variation in the specimen

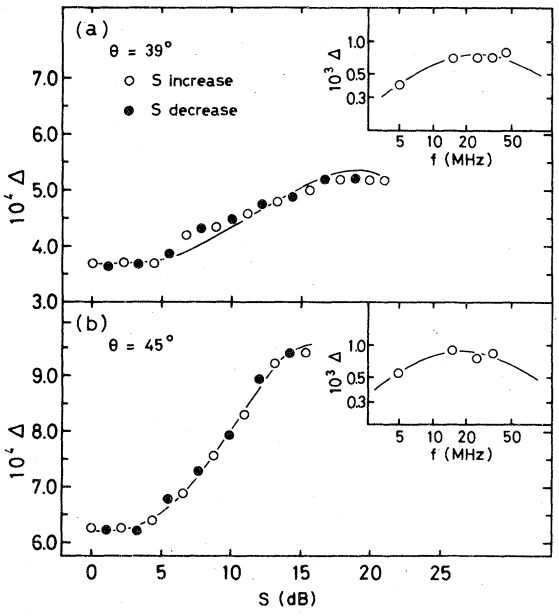

FIG. 6. Amplitude dependence of decrement. The abscissas are the relative values of the amplitude. Inserted figures show the frequency dependence of the decrement. Curves in these figures represent the theoretical ones.

was observed when S was changed. Inserted figures show the frequency dependence of decrement for the specimens measured at the lowest amplitude. Note that the lowest amplitude is always used in experiments other than the amplitude dependence experiments.

The amplitude dependence of decrement in crystals of ordinary materials often orginates from the breakaway of dislocations from impurity atoms.[18] In helium crystals, however, the number of impurity pinning points is too small. It is difficult to assume that the network length of dislocations is altered by the stress of sound waves and that the observed amplitude dependence is produced, since the network pinning is very stable. The reversible amplitude dependence also excludes the possibility of temperature effect which might be produced by the input energy of sound waves. In the next paragraph, the present experimental results will be analyzed by the "jog-depinning" mechanism.

G. Hysteresis loss

A theory of hysteresis loss is proposed as follows. When an external stress is applied, dislocations attempt to move the pinning jogs. The jog is able to move in the $\langle 1\bar{2}10\rangle$ direction conservatively, but the motion is opposed by the Peierls force for the jog. When the stress becomes large enough, irreversible motion of the jog or jog depinning occurs. For large alternating stress, a hysteresis-type loss of vibrational energy arises.

The jogs are randomly distributed on dislocations. Let us consider a part of the dislocations which has three jogs on it, namely, a jog on each of its ends and a jog in the middle of the two jogs. We call it a dislocation "segment". As can be seen later, jog depinning occurs at the middle jog when the length of the segment is fairly large. Therefore we take only long segments into account. Then the end jogs can be justifiably regarded as being fixed, because the probability of a long segment adjoining another long segment is not large. Let the distances between the end jogs and the middle jog be l_1 and l_2. When the middle jog moves the distance x from its equilibrium position, the increase of the potential energy of the dislocation segment is

$$U(x) = C\{[(l_1^2+x^2)^{1/2}-l_1] + [(l_2^2+x^2)^{1/2}-l_2]\} + (af/2\pi)[1-\cos(2\pi x/a)] \quad , \tag{12}$$

where C is the dislocation line tension, a is the lattice parameter, and f is the jog Peierls force. Here a sinusoidal Peierls potential is assumed. The first term of $U(x)$ is approximated by $\frac{1}{2}Cx^2(l_1^{-1}+l_2^{-1})$, since $l_1, l_2 >> x$. The force required to move the jog by distance x is then

$$F(x) = Cx(l_1^{-1}+1_2^{-1}) + f\sin(2\pi x/a) \quad . \tag{13}$$

The shapes of $U(x)$ and $F(x)$ are drawn in Fig. 7(a). When the second terms in $U(x)$ and $F(x)$ are large compared with the first terms, the maxima and minima in U are located at $x \approx na$ and $\frac{1}{2}na$, and those in F at $x \approx (n+\frac{1}{4})a$ and $(n-\frac{1}{4})a$, where n is an integer. The extrema, however, appear when a value of x which satisfies $dF/dx = 0$ exists. The condition is

$$(aC/2\pi f)(l_1^{-1}+l_2^{-1}) \leq 1 \quad , \tag{14}$$

namely, only long segments need be considered in the following discussion. When an external stress is applied to a dislocation, the force $F(x)$ is balanced by the force acting on the jog

$$F^* = \tfrac{1}{2}\sigma b(l_1+l_2) \quad , \tag{15}$$

where σ is the resolved shear stress exerted on the dislocation line. Now an alternating stress is considered. When the stress is increased, $F(x)$, and accordingly x, increase. The value of x jumps when F reaches a maximum [see Fig. 7(a)]. The nth jump occurs (e.g., $B \rightarrow C$) when the following condition is satisfied:

$$F((n-\tfrac{3}{4})a) = F^* \quad . \tag{16}$$

In the case of decreasing stress, the nth reverse jump

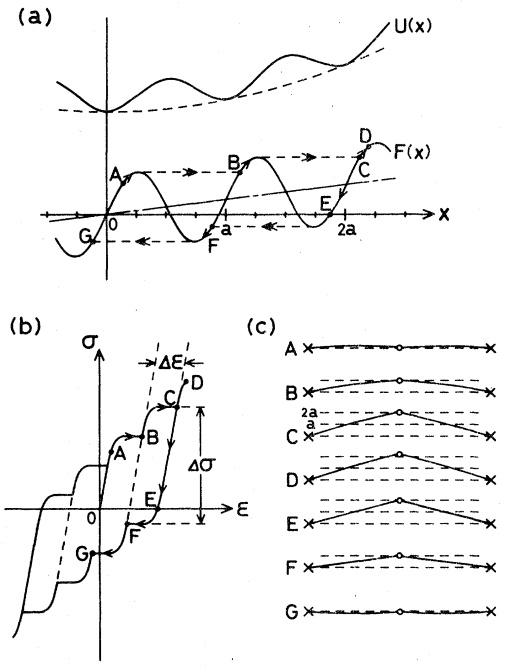

FIG. 7. Jog depinning and hysteresis loss.

(e.g., $E \rightarrow F$) occurs when

$$F((n-\tfrac{1}{4})a) = F^* \quad . \tag{17}$$

The strain produced by the dislocation movement is

$$\epsilon = bx(l_1 + l_2) \quad . \tag{18}$$

The stress σ versus strain ϵ thus shows hysteresis as drawn in Fig. 7(b). The movement of the dislocation segment is illustrated in Fig. 7(c). The letters A to G in these figures correspondingly represent typical states in the hysteresis. The energy loss arising from the hysteresis is approximated as

$$\Delta E = 2 \sum_{n>0} (\Delta\epsilon)_n (\Delta\sigma)_n \quad , \tag{19}$$

where $\Delta\epsilon$ and $\Delta\sigma$ are the quantities as shown in Fig. 7(b) and the suffix n refers to the nth jump. The values of $\Delta\epsilon$ and $\Delta\sigma$ can be calculated using Eqs. (16)–(18). The rounded shoulders of the hysteresis loops shown in the figure originate from the sinusoidal Peierls potential. The error in ΔE arising from this effect is estimated to be less than 10%. The quantity ΔE is really a function of l_1 and l_2, and the total loss is obtained as

$$\Delta E_{\text{tot}} = \int\int \Delta E N(l_1, l_2,)\, dl_1 dl_2 \quad , \tag{20}$$

and here $N(l_1, l_2)\, dl_1\, dl_2$ is the number of the segments with the lengths between l_1 and $l_1 + dl_1$; l_2 and $l_2 + dl_2$. The detailed calculation of ΔE_{tot} is shown in Appendix B. The decrement is then represented as

$$\Delta = \Omega \Delta E_{\text{tot}} / 2E; \quad E = \tau^2 / 2G \quad , \tag{21}$$

where Ω is the orientation factor and E is the vibrational energy. The stress τ is that applied to the specimen, and is related to the resolved shear stress σ as $\sigma = R\tau$, where R is the resolved shear stress factor. In the present experiment, the absolute values of the stresses are not known, and they are proportional to the voltage applied to the ultrasonic transducer. We here put $\sigma = kS$, where k is an unknown constant and S is the relative amplitude measured in the experiment. The final expression for the decrement from hysteresis loss is

$$\begin{aligned} \Delta_h &= (c_1 S^{-5/2} + c_2 S^{-2}) \exp(-c_0 S^{-1/2}) \quad ; \\ c_0 &= [(2C)^{1/2}/L] k^{-1/2} \quad , \\ c_1 &= [4aG(2C)^{1/2} R^2 \Omega / L^2](K\Lambda) f k^{-5/2} \quad , \\ c_2 &= (4aGR^2\Omega / L^2)(K\Lambda)(fL - aC) k^{-2} \quad . \end{aligned} \tag{22}$$

Here K is a constant which appears in the procedure of calculating ΔE_{tot} (see Appendix B). In the above formulas, L can be calculated from Eqs. (9) and (10), Ω is calculated as shown in Appendix A. The resolved shear stress factor is represented as $R = \cos\theta \sin\theta \cos\phi$, where θ is the angle between the c axis and the sound propagation direction, and ϕ is the angle between the slip direction and the projection on the slip plane of the sound propagation direction. After assuming uniform distribution of dislocations in three slip systems, the average value $\langle R^2 \rangle$ can be calculated. The unknown quantities in Eq. (22) are thus k, f, and $K\Lambda$. The total decrement of the specimen is

$$\Delta = \Delta_r + \Delta_h \quad , \tag{23}$$

where Δ_r is the decrement from resonance loss which is independent of amplitude.

By fitting the experimental data of the amplitude dependence to Eqs. (22) and (23), the constants Δ_r, c_0, c_1, and c_2 have been determined. The curves in Fig. 6 have been fitted, and the fitting is excellent. In Table II the determined values of the constants are shown for four specimens together with the calculated values of $\langle R^2 \rangle$ and Ω. Using these values one can determine two unknowns k and f. The constant K is calculated when the k and f are known (see Appendix B), and finally the values of Λ can be obtained. The results are shown also in Table II.

TABLE II. Constants and quantities determined from the amplitude dependence of decrement for four specimens.

θ (degree)	36	38	39	45
$10^4 \Delta_r$	4.47	4.05	3.68	6.20
c_0	19.5	12.9	17.3	15.3
c_1	41.3	3.68	21.2	29.6
c_2	−7.78	−0.745	−3.21	−6.43
$\langle R^2 \rangle$	0.038	0.039	0.040	0.042
Ω	0.094	0.10	0.11	0.13
k (10^2 dyn/cm^2)	1.3	2.9	1.6	2.1
f (10^{-10} dyn)	5.0	6.3	6.5	5.5
Λ (10^9 cm^{-2})	6.3	3.2	3.3	6.4
Λ_{freq} (10^9 cm^{-2})	3.1	3.1	6.1	6.8

The Λ_{freq} in the last line of the table represents the dislocation density independently determined from the frequency dependent decrement of the specimens. Specifically, Eq. (6) has been fitted to the data as shown in the inserted figures of Fig. 6, and the values of Λ_{freq} were determined from the peak height by using the calculated value of L after assuming an exponential distribution of pinning points.

The obtained results will be considered in the following. The scatter of the values of f among specimens is not large, which is reasonable because the jog Peierls force should be the same. The average of f is 5.8×10^{-10} dyn. The jog Peierls stress is calculated as $\sigma_J = f/bb' \approx f/b^2$, and the ratio σ_J/G is 3.0×10^{-3}. For dislocations on the slip plane in usual close-packed crystals, the ratio is considered to be 10^{-4} or less.[24] It is reasonable that the ratio is larger for the jog Peierls stress, since jogs are dislocations which are hard to move. There is a satisfactory agreement between the dislocation densities independently derived from the amplitude dependence and the frequency dependence. This fact shows that the present method of analysis is reliable. A dislocation density of the order of 10^9 cm^{-2} is not unreasonable, because helium crystals are very soft and may be easily strained during the crystal growth. Finally, from the values of k the stresses in the specimens can be calculated. The resolved shear stress σ is $2 \times 10^2 - 2 \times 10^3$ dyn/cm^2 for $S = 1-10$. Then the stress and strain along the sound propagation direction are 10^3-10^4 dyn/cm^2 and $2 \times 10^{-6} - 2 \times 10^{-5}$, respectively. Moreover, in usual MHz pulse ultrasonic experiments the displacement amplitude produced in the specimen by a quartz transducer is shown to be $10^{-8}-10^{-7}$ cm when a voltage of 100–1000 V is applied.[26] The strain amplitude is estimated after dividing the displacement by half of the wave length of the sound, and the amplitude is $10^{-6}-10^{-5}$ in the case of helium crystals. This value is in agreement with the above result. It is noted that the strain amplitude is large in soft crystals and amplitude dependence experiments can successfully be made.

It can be concluded here, from the time dependence and the amplitude dependence experiments, that (i) the dominant pinning points on dislocations are jogs, and (ii) the pinning length can be calculated from the concentration of jogs in thermal equilibrium.

H. Temperature dependence

The frequency dependence of attenuation in crystals has been measured at successively higher temperatures between 1.38 and 2.25 K. Each attenuation-versus-frequency measurement was made after keeping the temperature constant within 1 mK for 30 min. Between successive measurements the temperature was increased slowly (less than 1 mK/min), because the attenuation was unreasonably increased when the temperature was changed rapidly. The data at each temperature were fitted to the overdamped resonance formulas Eq. (6). Two quantities f_m and Δ_m were found to be dependent on temperature. The dislocation density Λ and the damping constant B were determined as functions of temperature, where an exponential distribution of pinning points was adopted and the pinning lengths were calculated from Eqs. (9) and (10). Experiments were made for three 20.5 cm^3/mole crystals and three 19.2 cm^3/mole crystals, and the results were as shown in Figs. 8 and 9.

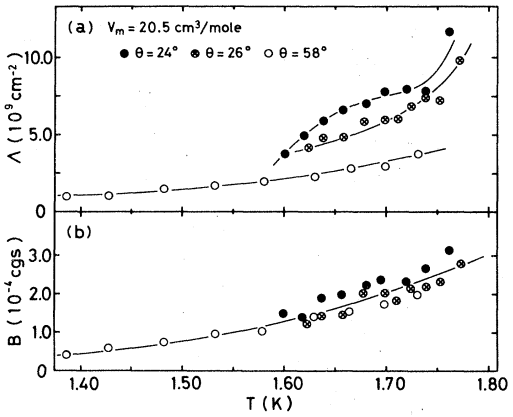

FIG. 8. Temperature dependence of dislocation density (a) and damping constant (b) for different crystals with molar volume of 20.5 cm^3/mole. The curve in (b) represents the result of parameter fit.

The dislocation density Λ increases with temperature, but the temperature dependence is different in

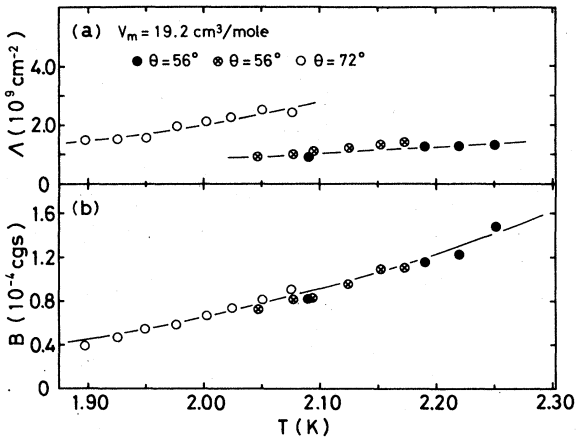

FIG. 9. Temperature dependence of dislocation density and damping constant for crystals with molar volume of 19.2 cm^3/mole.

TABLE III. Constants and quantities concerning damping constant for two molar volumes.

V_m (cm^3/mole)	20.5	19.2
B_0 (cgs)	0.235	0.0709
E_B (K)	12.0	14.1
Θ_D/E_B	2.1	2.0
N_v (10^{22} cm^{-3})	2.9	3.1
c (10^4 cm/sec)	2.46	2.89
Q (10^9 dyn/cm^2)	5.2	4.9
Q/G	35	23

every specimen. This may be explained as follows. The helium crystal is in a specimen cell and has no free surfaces, and the temperature of the crystal is changed under the condition of constant volume. Then thermal stresses are produced and dislocation sources are activated in the specimen. The dislocation density is thus increased, and its change depends on the details of the thermal stresses and the dislocation sources.

The damping constant B increases with temperature. It is important that the data for different specimens fall on a common curve when the molar volume of the specimens is the same. This result is reasonable, because the damping constant for dislocation movement in pure materials is considered to be an intrinsic quantity of the crystal. It was found that the temperature dependence of the damping constant was well expressed by the relation

$$B = B_0 \exp(-E_B/T) \quad . \tag{24}$$

The curves in Figs. 8(b) and 9(b) have been fitted, and the determined values of the constant B_0 and E_B are in Table III. Interpretation of the results will be made in the next paragraph.

I. Damping constant

There are many theories on the damping constant for dislocation motion in insulating crystals.[21,27–31] The magnitude and also the temperature dependence of the damping constant determined in the present experiment cannot be explained by these theories. For example, anharmonicity theory[30] gives the temperature dependence $B \propto T^5$ and the magnitude $B = 1 \times 10^{-11}$ cgs at 1.7 K for a hcp ^{4}He crystal with molar volume of 20.5 cm^3/mole, and fluttering theory[31] gives the dependence $B \propto T^3$ and the magnitude $B = 6 \times 10^{-7}$ cgs. The present authors propose a new mechanism of dislocation damping in the following.

In the vicinity of a lattice defect, the atomic configuration and the interatomic force constants are very different from those in a perfect lattice, and the state of atomic vibration may also be different. We assume that there exists a lattice vibrational state spatially localized near the dislocation core, and the state has a vibrational frequency ω_0 which is lower than the Debye frequency of the lattice. Let the state be called the quasilocal mode of phonons. The mode is regarded as a standing wave enclosed in a limited region around the dislocation line, and the wave is composed of two waves with propagation vectors normal to the dislocation line and opposite to each other in direction. For a uniformly moving dislocation, the frequency of the quasilocal phonons should split into two because of the Doppler effect: namely, the frequency ω_0 changes to $\omega_0 \pm \Delta\omega = \omega_0 \pm \omega_0(v/c)$, where v is the velocity of the dislocation movement and c is the sound velocity. This state is realized for quasilocal phonons by absorbing and emitting thermal phonons in the crystal through the three-phonon processes. The processes are

$$\begin{aligned} &(\omega_0) + (\Delta\omega) \rightarrow (\omega_0 + \Delta\omega) \quad , \\ &(\omega_0) \rightarrow (\Delta\omega) + (\omega_0 - \Delta\omega) \quad , \end{aligned} \tag{25}$$

where $\Delta\omega$ represents the frequency of the thermal phonons. Let the numbers of the first and the second processes occurring in unit time per unit length of dislocation be P_1 and P_2. The energy transferred from the quasilocal phonon system to the crystal in unit time is

$$W = \hbar\Delta\omega(P_2 - P_1) \quad . \tag{26}$$

The values of P_1 and P_2 can be obtained using a quantum-mechanical method.[32] The energy W is required to move the dislocation with the quasilocal phonons. The force acting per unit length of moving dislocation is by definition equal to $F = Bv$. Then the energy dissipated in unit time is $Fv = Bv^2$, which should be equal to W. Accordingly, the damping constant B can be calculated as:

$$B = W/v^2 \quad . \tag{27}$$

The wave vectors of quasilocal phonons are, however, not necessarily parallel to the direction of the dislocation movement, and the above value for B should be multiplied by an averaging factor $2/\pi$. The final expression for the damping constant is shown to be

$$B = \frac{\hbar^2\omega_0^6 N_v r^2 Q^2}{6\pi\rho^3 c^{11}} \exp(-\hbar\omega_0/k_B T) \quad , \tag{28}$$

where ρ is the material density, c is the sound velocity, N_v is the number of atoms per unit volume of the crystal, r is the radius of a cylindrical region in which the quasilocal phonons exist, and Q is a constant representing the crystal anharmonicity. In the continuum approximation, Q is expressed as a combination of second- and third-order elastic constants.[33] The derivation of Eq. (28) is shown in Appendix C.

The above theoretical formula, Eq. (28), shows the same temperature dependence as the experimental relation, Eq. (24). As shown in Table III, it can be seen that the experimental value of E_B is just half of the Debye temperature, Θ_D. This means that the frequency of the quasilocal phonons is half that of the Debye frequency, and the wavelength is four times the lattice parameter a. Accordingly, the quasilocal phonons are considered to exist in a cylindrical region of radius $2a$ around the dislocation line. This conclusion seems to be reasonable since the atomic configuration is much distorted in the dislocation core and the diameter of the core is usually considered to be several times the lattice parameter. By comparing the experimental value of B_0 with preexponential factor in Eq. (28), one can determine the value of the anharmonicity constant Q. Here we use the relation $r=2a$ and $\omega_0=k_B E_B/\hbar$, and also other constant values tabulated in Table III or Table I. We adopted the sound velocity c for the slow transverse sound propagating in the basal plane of the crystal (see Appendix C). The thus-determined values of Q are listed in Table III. The last line shows the ratio of Q to the shear modulus G. These results are very reasonable, because Q is a combination of the second- and the third-order elastic constants and is expected to be an order of magnitude larger than the second-order elastic constants.[9] The quantity Q/G is considered to be representative of the crystal anharmonicity. It is understandable that the value is smaller for crystals with smaller molar volume, because the lattice anharmonicity is reduced in more closely packed crystals. Finally, it is noted that the damping mechanism considered here is important for materials with small sound velocities.

The experimental results on the damping constant are consistently explained by the mechanism of quasilocal phonon damping. The actual existence of the quasilocal phonons, however, is the problem. The present authors used the same idea to analyze their experiments on the low-temperature thermal conductivity and specific heat in crystals with dislocations,[34] and obtained reasonable success in the analysis. Further experimental studies to verify the reality of quasilocal phonons are now being scheduled. There are several theoretical studies on the phonon modes in dislocated crystals.[35] These theories, however, are not directly concerned with our quasilocal phonon model. Much more experimental and theoretical investigations are required to justify the present proposition for the damping mechanism.

IV. DISCUSSION

In this section, three subjects will be taken up. First, experimental studies on the attenuation of acoustic phonons, ultrasound, and mechanical oscillation in solid helium made by other investigators are briefly mentioned. This review is closely related to the following discussion. Second, the possible sources of sound attenuation in solid helium other than dislocation damping are fully discussed. The purpose is to consider whether the present experimental results are explained by other mechanisms. Third, experimental and theoretical studies concerning dislocations in helium crystals are described and compared with the present study.

A. Attenuation experiments

The attenuation of GHz phonons has been measured as a function of temperature in hcp ^{4}He by Dransfeld, Hunklinger, and co-workers,[36,37] where the lifetime of longitudinal phonons generated by the stimulated Brillouin scattering was determined by an optical method. The attenuation showed approximately a T^4 temperature dependence, and was attributed to three-phonon processes between acoustic and thermal phonons. A comparison with the Landau-Rumer theory gave satisfactory agreement with the data. They also found that the third-order elastic constants of the helium crystal were an order of magnitude larger than the second-order elastic constants.

The measurement of ultrasonic attenuation by the pulse echo method has presented great experimental difficulties, and only qualitative studies have been made at the early stage.[38] Recently two papers appeared, which were presented by Calder and Franck[39] and Iwasa *et al.*[40] Both of them measured the attenuation of MHz longitudinal ultrasonic waves of three frequencies as a function of temperature in hcp ^{4}He crystals, and their experimental results have many common features. Iwasa *et al.* considered that the origin of the attenuation was the crystal dislocations. Franck *et al.* tended to interpret their results as being due to phonon interactions, but had no definite conclusion.

Two relaxation maxima have been observed by Andronikashvili *et al.*[41] in the temperature dependence of low-frequency damping for transverse oscillation of solid helium in a capillary. They suggested that the origin of the relaxation was the movement of defectons in helium crystals, but a detailed discussion was not presented. Tsymbalenko has measured the damping of oscillation of a kHz quartz resonator frozen into solid helium in a cell.[42] The temperature dependence of the logarithmic decrement and its dependence on the strain amplitude of the resonator were studied. Dislocation damping was considered in order to interpret the experimental results.

B. Sources of attenuation

When specimen crystals are polycrystalline, sound attenuation arises from the scattering of the wave by

grain boundaries. There are two cases for the scattering, namely, Rayleigh scattering for $R < \lambda/2\pi$ and stochastic scattering for $R > \lambda/2\pi$, where R is the dimension of the grains and λ is the wavelength of sound. The attenuation is respectively proportional to R^3f^4 and Rf^2, where f is the sound frequency. For the case of $f=5$ MHz and the sound velocity $c=500$ m/sec in helium crystals, $\lambda/2\pi=1.6\times10^{-3}$ cm. The solid helium grown under constant pressure crystallizes into a single crystal or a few large crystals, and in the latter case the grains are as large as several mm.[43] Thus stochastic scattering may occur in polycrystalline helium. The attenuation is then expressed as[44]

$$\alpha=\frac{16\pi^2}{1575}\frac{Rf^2}{\rho^2c^6}F \ , \tag{29}$$

where ρ is the density and F is a function of elastic constants of crystal. For $f=5$ MHz, $R=10^{-1}$ cm, and $\rho=0.20$ g/cm^3 for molar volume of 20.5 mole/cm^3, the decrement in the helium crystal should be $\Delta=0.74$. This value is very large compared with the experimental values of $\Delta=(5-15)\times10^{-4}$ in the specimens we used. Extremely large attenuation was observed in some of the crystals grown, and they were considered to be polycrystals. We have not used such crystals in the attenuation measurements.

One origin of ultrasonic attenuation is the thermoelastic effect, which arises from a production of entropy and a dissipation of energy accompanied by heat flow between the compressed and expanded regions in a wave-propagating solid.[9] The loss is of the relaxation-type and its expression for a hexagonal crystal is

$$\Delta=\frac{\pi T}{C_p}\frac{[(c'_{11}+c'_{12})\beta'_{\perp}+c'_{13}\beta'_{\parallel}]^2}{c'_{11}}\frac{\omega\tau}{1+\omega^2\tau^2} \ , \tag{30}$$

where T is the temperature, C_p is the isobaric specific heat, c'_{ij} is the elastic constant when the sound propagation direction is chosen as a coordinate axis, $\beta'_{\perp}=\beta_{\perp}\cos\theta+\beta_{\parallel}\sin\theta$, $\beta'_{\parallel}=\beta_{\parallel}\cos\theta+\beta_{\perp}\sin\theta$, and here $\beta_{\perp}$ and $\beta_{\parallel}$ are the thermal-expansion coefficients perpendicular and parallel to the c axis, and θ is the orientation angle. The relaxation time for the present case is $\tau=D/c^2=\kappa/\rho C_v c^2$, where D is the thermal diffusivity, κ is the thermal conductivity, and C_v is the specific heat under constant volume. By using the values $C_v\approx C_p=3.86\times10^5$ erg/K cm^3 calculated from the Debye temperature and $\kappa=5.0\times10^{-3}$ W/K cm,[45] it is shown that the decrement has its maximum value at a frequency of 6.1×10^8 Hz. Accordingly, the peak in the decrement versus frequency in the present experiment is not due to the thermoelastic effect. The decrement at $f=5$ MHz and $T=1.7$ K is estimated by using $\beta_{\perp}\approx\beta_{\parallel}\approx1.43\times10^{-3}$ K^{-1}, and the value is $\Delta=3.4\times10^{-4}$. This may be an overestimated value, since we calculated the thermal-expansion coefficient from the thermodynamical quantities on the melting curve.[46] We consider that the contribution of the thermoelastic effect is not so large in the present attenuation measurements.

Ultrasound is attenuated through the interactions with thermal phonons, and the interactions are caused by the anharmonicity of the crystal lattice.[9] There are two kinds of theoretical approach, namely, the Landau-Rumer-type and the Akhieser-type. They are respectively adopted when $\omega\tau$ is larger or smaller than unity, where τ is the lifetime of thermal phonons and ω is the sound frequency. Landau-Rumer attenuation has been actually observed in solid helium in GHz range. In the present MHz experiment at temperatures above 1 K, it turns out that $\omega\tau\ll1$ by using the value of $\tau\approx6\times10^{-10}$ sec estimated from the thermal conductivity in the umklapp region.[45] The expression for the Akhieser-type loss derived, for example, by Guyer is[47]

$$\Delta=\frac{2\pi^2\gamma^2\kappa fT}{3\rho c^4} \ , \tag{31}$$

where γ is the Grüneisen parameter, and other symbols have the same meanings as before. The value of γ in solid helium has been determined by several investigators using various methods, and the value was in the range of 2–3.[16] When $\gamma=2.5$ is adopted, then $\Delta=1.4\times10^{-5}$ at $f=5$ MHz and $T=1.7$ K. After considering the frequency dependence and the magnitude of the decrement, it is concluded that phonon damping is not the main origin of the attenuation in the present case. Also shown by Guyer was that a resonant enhancement of attenuation would appear in the second-sound region $\tau_N\ll\omega^{-1}\ll\tau_R$, where τ_N and τ_R are the relaxation times for the normal and the umklapp processes. However, the second-sound criterion is not realized under the present experimental conditions (see Fig. 1 in Ref. 47).

Extensive arguments are now being made on the delocalized point defects or defectons in quantum crystals.[4] The energy dissipation arising from the movement of defectons[48,49] and bidefectons[50] has been precisely discussed by Meierovich. He described the sound absorption due to diffusion flow of defectons in momentum space in the absence of particle flux in coordinate space. The expression for the decrement is[49]

$$\Delta=\left(\frac{I}{T}\right)\exp\left(-\frac{\epsilon_0}{T}\right)\frac{\omega\tau}{1+\omega^2\tau^2} \ , \tag{32}$$

where I is a quantity independent of temperature, and ϵ_0 is the energy gap in the energy spectrum for defectons. The relaxation time τ is determined from the defecton-phonon interactions and is shown to be

proportional to T^9. Meierovich cited our experiment[6] and noted that our data were in agreement with his theory. We must say, however, that our result on the temperature dependence of the decrement cannot be explained by his theory. For example, note the data in Figs. 2(b) and 2(c) and note the height Δ_m and the location f_m of each peak. Changes of these quantities with temperature are $\Delta_m(1.70\ \text{K})/\Delta_m(1.39\ \text{K}) = 0.64$ and $f_m(1.70\ \text{K})/f_m(1.39\ \text{K}) = 1.13$, while they should be 3.0 and 0.16 from the theory when $\epsilon_0 = 10$ K is used. We feel that the theory is rather suited to interpret the experimental result by Andronikashvili *et al.*[41]

C. Dislocations in helium crystals

An unusual temperature dependence of specific heat was sometimes suggested in hcp ^{4}He. The anomaly was represented by a term proportional to temperature in addition to the usual Debye T^3 term. Franck[51] observed that the anomaly was reduced by the factor $\frac{1}{3}$ for annealed samples, and mentioned that the vibration of pinned dislocations might contribute to the linear term at low temperatures.[52] The linear term was also detected in bcc ^{3}He crystals.[53] These anomalies were, however, not observed by other authors.[54,55] Our feeling is that the densities of dislocations are very different among specimens grown by different authors. In the case of thermal conductivity of solid helium, the effect of annealing has also been found.[45] Detection of dislocations in helium crystals through their thermal properties is an interesting subject, and crystals containing relatively high density of dislocations may be required for that purpose.

The mechanical properties of solid helium were first investigated by Andreev *et al.*[56] They froze a small steel ball into solid helium and observed its motion in a magnetic field. They intended to find superfluidity of the crystal originating from the motion of zero-point defectons. Suzuki studied the plastic deformation of polycrystalline hcp ^{4}He by measuring the force to move a ball or a rod in solid helium,[57] and concluded that the plastic flow was primarily due to motion of dislocations. He observed that the force-displacement curve revealed a marked yield drop followed by a steady-state flow. His argument was that the sharp yield was similar to that seen in covalent crystals, and that the Peierls stress for nonbasal slip of dislocations might be very large. He also analyzed steady plastic flow and estimated the damping constant for the dislocation motion. The value was at least $B = 4.0 \times 10^{-3}$ cgs at 2.1 K for crystals under the pressure of 29–51 atm. Tsymbalenko measured the yield stress of hcp ^{4}He contained in an ampoule by applying pressure on the wall.[58] He stated that the plasticity of solid helium was similar to that of ordinary materials, especially of solidified inert gases. The plastic deformation of freestanding unconstrained single crystals of hcp and bcc ^{4}He was studied by Sanders *et al.*[59] The method was such that a crystal of solid helium surrounded by fluid helium on its side faces was prepared by controlling the temperature gradient in the specimen. They observed very small constant flow stress. If the value corresponded to the Peierls stress σ_P as they imagined, then the value of σ_P/G was 10^{-4} or less. They also monitored the deformation of the crystal by observing the ultrasonic attenuation in the specimen. In the case of hcp ^{4}He crystals, the attenuation in the undeformed specimens had values comparable to those measured by the present authors. The attenuation increased rapidly when the crystal was deformed, and they considered that dislocations were multiplied by the deformation. In the meanwhile, they argued that the plastic deformation of bcc ^{4}He might not originate from motion of dislocations. After all it is concluded that, at least in the case of hcp ^{4}He crystals, there exist dislocations which move rather easily and produce plastic deformation.

Wanner *et al.*[60] and Iwasa *et al.*[40,61] observed an anomalous temperature dependence of sound velocity in hcp He below 1 K. The anomaly is very small above 1 K, and is overwhelmed by the phonon part of the velocity change. They analyzed their data by the Granato-Lücke theory and obtained typical values of the dislocation density $\Lambda = 10^6$ cm^{-2}, the pinning length $L = 5 \times 10^{-4}$ cm, and the damping constant $B = 3 \times 10^{-7} T^3$ cgs. They concluded that the pinning is due to network pinning, and the damping is mainly due to the fluttering mechanism.[31] We here present interesting curves in Fig. 10. The damping constant from the quasilocal phonon mechanism B_L and the damping constant from the fluttering mechanisms B_F are shown as functions of temperature in Fig. 10(a), and the jog pinning length L_J and the network pinning length L_N are shown in Fig. 10(b). Here B_L and L_J are values for $V_m = 20.5$ cm^3/mole and B_F and L_N are those given by Iwasa *et al.*[40] It is seen that $B_L \gg B_F$ and $L_J \ll L_N$ above 1 K, and the situation is reversed below about 0.7 K. It is considered that our model of the dislocation damping can be applied above 1 K, while another model might be taken for lower temperatures. The densities of dislocations determined in our study and in their study are also different. This is not so critical, because dislocation densities in specimens grown by different methods may be widely different. Iwasa *et al.*[40] also presented data on the temperature dependence of attenuation, which seem, however, to be preliminary. Tsymbalenko[42] observed a peak in the decrement-versus-temperature curve for hcp ^{4}He, and analyzed the results by the Granato-Lücke theory. As can be seen from the overdamped formula, such a peak should appear at a certain temperature when the damping

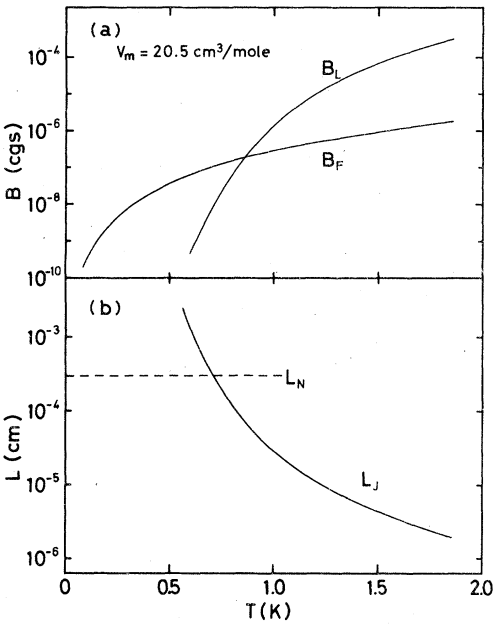

FIG. 10. Calculated values of damping constant (a) and pinning length (b).

constant changes with temperature. Further, we must mention that he finds no strain amplitude dependence of the decrement. However, the values of the strain amplitude estimated by the author seem to be those in the quartz resonator, and the strain really produced in solid helium is considered to be small in his experiment.

Existing theories of dislocations in a quantum crystal will be mentioned briefly. Andreev[62] considered the case of a dislocation positioned in the slip plane at a certain angle to the crystallographic directions. There are a certain number of kinks on the dislocation, and in a quantum crystal each kink is regarded as a quasiparticle with one-dimensional quasimomentum. Just as in the case of defectons in the crystal, the quantum-mechanical delocalization of kinks occurs, which leads to delocalization of the dislocation in the slip plane. This is, however, not the case of a dislocation line which is in a Peierls potential valley and anchored by pinning points, and only such dislocations can be the origin of the overdamped loss observed in the present experiments. Petukhov and Pokrovskii[63] proposed a theory of the tunneling motion of a dislocation situated in the Peierls potential valley. The motion of dislocation results from creation of kink pairs, and at that time the part of the dislocation line between the kinks migrates to the adjacent valley through the potential barrier by quantum-mechanical tunneling. The tunneling occurs under the action of an external stress, and the transition probability is not so large when the stress is small. In the attenuation experiments, the stress produced by sound may not be so large as to cause the tunneling motion of dislocations.

V. CONCLUSION

Ultrasonic attenuation in solid helium has been measured by the pulse reflection method, where pulse echo patterns of good quality were obtained owing to a carefully prepared sample cell. The values of attenuation are considered to represent true mechanical energy dissipation in the specimen since other losses of acoustic origin are estimated to be small. A number of specimens have been grown under constant pressure, and specimens used for the attenuation measurements are considered to be single crystals. The overdamped resonance of crystal dislocations is the main origin of the attenuation, and the slip plane of the dislocations is the basal plane. Other sources of sound attenuation are shown not to account for the experimental results. Under the present experimental condition, the dominant pinning points for dislocations are jogs, and the pinning length is determined from their thermal equilibrium concentration. A mechanism of damping of dislocation motion has been proposed, namely, the energy loss due to three-phonon processes between thermal phonons and quasilocal phonons around dislocations. The high concentration of jogs and the enhancement of the quasilocal phonon damping both result from the smallness of sound velocities or elastic constants in helium crystals, which is a reflection of the quantum nature of the crystal. Aside from these points, the analysis of the experiments has been made on the basis of the classical theory of dislocation damping. However, the possibility of finding a quantum character of the dislocations in solid helium is not denied, which is a problem to be studied in the future.

ACKNOWLEDGMENTS

The authors wish to express their gratitude to Dr. A. V. Granato, Dr. R. A. Guyer, Dr. A. Hikata, Dr. H. Suzuki, and Dr. T. Mori for their interest and many valuable suggestions; to Dr. D. C. Worth for reading the manuscript; and also to Dr. Y. Kogure, S. Mori, S. Araki, T. Kosugi, S. Arakawa, and Y. Shimizu for their cooperation and help.

APPENDIX A: ORIENTATION FACTOR

Orientation factor for dislocations on the kth slip system Ω_k is defined as

$$\Delta = \sum_k \Omega_k \Delta_k \ , \tag{A1}$$

where Δ_k is the decrement due to the dislocations on the kth slip system, and Δ is the total decrement of the specimen. The decrements are defined by

$$\Delta = \Delta E/2E, \quad \Delta_k = \Delta E_k/2E_k \ , \tag{A2}$$

where E and E_k are the vibrational energies and ΔE and ΔE_k are the energy losses per cycle. The relation

$$\Delta E = \sum_k \Delta E_k = \sum_k \left(\frac{\tau_k^2}{G_k}\right)\Delta_k \tag{A3}$$

holds since $E_k = \tau_k^2/2G_k$, where τ_k and G_k are the shear stress and the shear modulus along the kth slip direction. From these relations one obtains

$$\Omega_k = \tau_k^2/2G_k E \ , \tag{A4}$$

and the orientation factor of the specimen is

$$\Omega = \left(\frac{1}{k}\right)\sum_k \Omega_k \ , \tag{A5}$$

when dislocations are uniformly distributed on all slip systems.

For a traveling plane wave propagating along the (l,m,n) direction with the polarization direction (α, β, γ), the displacement components are

$$\begin{aligned} &s_1 = \alpha\psi, \quad s_2 = \beta\psi, \quad s_3 = \gamma\psi \ ; \\ &\psi = A_0 \exp i\,[\omega t - q(lx + my + nz)] \ . \end{aligned} \tag{A6}$$

Then the kth orientation factor is given as

$$\Omega_k = (\tau_k^*)^2/2G_k E^* \ , \tag{A7}$$

where τ_k^* and E^* are defined as

$$\tau_k = iq\psi\tau_k^* \ , \quad E = -q^2\psi^2 E^* \ . \tag{A8}$$

For a hexagonal crystal with the (0001) slip plane and the $[11\bar{2}0]$, $[\bar{1}2\bar{1}0]$, $[\bar{2}110]$ slip directions, $\tau_1 = (\frac{1}{2})\sigma_{yz} + (\frac{1}{2}\sqrt{3})\sigma_{zx}$, etc. Here the σ_{ij}'s are the stress components for the $[10\bar{1}0]$, $[\bar{1}2\bar{1}0]$, [0001] Cartesian coordinate axes. These components can be represented by the elastic constants and the strains ϵ_{ij} or displacement gradients, and finally it turns out that

$$\tau_1{}^* = [(\tfrac{1}{2})(\beta n + \gamma m) + (\tfrac{1}{2}\sqrt{3})(\alpha n + \gamma l)]c_{44} \ ,$$

etc. It is also shown that the shear moduli are $G_1 = G_2 = G_3 = c_{44}$. From these relations, the orientation factor of the specimen is obtained as

$$\Omega = (c_{44}/4E^*)[(\beta n + \gamma m)^2 + (\alpha n + \gamma l)^2] \ ; \tag{A9}$$

and by using the relation $E = \frac{1}{2}\sigma_{ij}\epsilon_{ij}$, it can be shown that

$$\begin{aligned} E^* = \tfrac{1}{2}\{&c_{11}[\alpha^2 l^2 + \beta^2 m^2 + \tfrac{1}{2}(\alpha m + \beta l)^2] \\ &- \tfrac{1}{2}c_{12}(\alpha m - \beta l)^2 + 2c_{13}\gamma n(\alpha l + \beta m) \\ &+ c_{44}[(\beta n + \gamma m)^2 + (\alpha n + \gamma l)^2] + c_{33}\gamma^2 n^2\} \ . \end{aligned} \tag{A10}$$

The polarization direction (α, β, γ) of the wave can be calculated by the usual method,[9] and Ω can be evaluated for any propagation direction.

APPENDIX B: CALCULATION OF AMPLITUDE DEPENDENCE

The factors in Eq. (19) are obtained from Eqs. (13) and (15)–(18) as

$$\begin{aligned} (\Delta\epsilon)_n &= b(l_1 + l_2)[(n + \tfrac{1}{4})a - (n - \tfrac{1}{4})a] \\ &= \tfrac{1}{2}ab(l_1 + l_2) \equiv \Delta\epsilon \ , \end{aligned} \tag{B1}$$

$$\begin{aligned} (\Delta\sigma)_n &= \frac{F((n - \frac{3}{4})a) - F((n - \frac{1}{4})a)}{\frac{1}{2}b(l_1 + l_2)} \\ &= \frac{2}{b(l_1 + l_2)}[2f - \tfrac{1}{2}aC(l_1^{-1} + l_2^{-1})] \equiv \Delta\sigma \ , \end{aligned} \tag{B2}$$

and are both independent of n. Thus Eq. (19) is reduced to

$$E = 2n\Delta\epsilon\Delta\sigma \ , \tag{B3}$$

where n is determined from Eq. (16) as an integer satisfying the relation

$$n \leqslant \frac{\frac{1}{2}b(l_1 + l_2)\sigma - f}{aC(l_1^{-1} + l_2^{-1})} + \frac{3}{4} \ . \tag{B4}$$

The distribution function of the dislocation segments is[18]

$$N(l_1, l_2) = (\Lambda/L^3)\exp[-(l_1 + l_2)/L] \ . \tag{B5}$$

The total loss ΔE_{tot} is calculated using these expressions.

The straightforward calculation is complicated, and at first the simple case of $l_1 = l_2$ $(= l)$ is considered. The total loss is

$$\begin{aligned} \Delta E_{\text{tot}} &= \sum_{n=1}^{\infty} n \int_{l_{(n)}}^{l_{(n+1)}} 2\Delta\epsilon(l_1 = l_2 = l) \\ &\quad \times \Delta\sigma(l_1 = l_2 = l)N(l)\,dl \\ &\equiv \sum_{n=1}^{\infty} n\,\Delta E_{(n)} \ . \end{aligned} \tag{B6}$$

Here $\Delta E_{(n)}$ is the contribution from the segments which jump n times in a quarter cycle of the alternating stress, $l_{(n)}$ is half the length of the segment, and $N(l)$ is the distribution function of the segment with length $2l$. With substitution of $l_1 = l_2 = l$ in Eq. (B4),

$$l_{(n)} = (1/2\sigma b)\{f + [f^2 + 8abC(n - \tfrac{3}{4})\sigma]^{-1/2}\} \quad . \tag{B7}$$

Expression for the distribution function $N(l)$ is derived as follows. The number of segments for which $l_1 = l_2 = l$ is $N(l)$. The total number of $N(l)$ when the l is varied from 0 to l_0 is

$$N_{\text{tot}}(l_0) = \int_0^{2l_0} dl_1 \int_0^{2l_0 - l_1} N(l_1, l_2)\, dl_2 \quad . \tag{B8}$$

Here $N(l_1, l_2)$ is the distribution function of Eq. (B5), and it turns out that

$$N_{\text{tot}}(l_0) = (\Lambda/L)[1 - e^{-2l_0/L} - (2l_0/L)e^{-2l_0/L}] \quad . \tag{B9}$$

By definition $N(l_0) = (d/dl_0)N_{\text{tot}}(l_0)$, and finally one obtains

$$N(l) = (4\Lambda/L^3)\, l \exp(-2l/L) \quad . \tag{B10}$$

Now it is assumed that (i) $f/b^2G \sim 10^{-3}$, i.e., $f \sim 2 \times 10^{-10}$ dyn, and (ii) $\sigma \sim 10^3$ dyn/cm^2. These assumptions are not indispensable ones, but they reduce the complexity of the calculation. The above assumptions are shown to be reasonable, as described in the text. Then the $l_{(n)}$ of Eq. (B7) is approximated as

$$l_{(n)} = [(2C/\sigma)(n - \tfrac{3}{4})]^{1/2} \quad . \tag{B11}$$

By using this expression, $\Delta E_{(n)}$ and ΔE_{tot} of Eq. (B6) are calculated as

$$\Delta E_{(n)} = [(X - Yl)e^{-2l/L}]_{W(n-3/4)}^{W(n+1/4)} \quad ,$$

$$\Delta E_{\text{tot}} = \sum_{m=0}^{\infty} [YW(m + \tfrac{1}{4})^{1/2} - X]\, e^{-2W(m+1/4)^{1/2}/L} \quad ,$$

$$X \equiv (4a\Lambda/L^2)(aC - fL) \quad ,$$

$$Y \equiv 8a\Lambda f/L^2, \quad W \equiv (2C/\sigma)^{1/2} \quad . \tag{B12}$$

When the above mentioned assumptions (i) and (ii) are adopted, the first term ($m = 0$) of the series representing ΔE_{tot} is shown to be extremely large compared to the successive terms. Then one obtains, with sufficient accuracy, the following expression:

$$\Delta E_{\text{tot}} = (4a\Lambda/L^2)[f(2C/\sigma)^{1/2} + (fL - aC)] \times \exp[-(2C/\sigma)^{1/2}/L] \quad . \tag{B13}$$

Actually, the case of $l_1 = l_2 = l$ is not realized. The above ΔE_{tot} is then corrected by multiplying by the constant K defined as

$$K = \frac{\int_0^1 n(\alpha)\Delta\epsilon(\alpha)\Delta\sigma(\alpha)\, d\alpha}{n(\tfrac{1}{2})\Delta\epsilon(\tfrac{1}{2})\Delta\sigma(\tfrac{1}{2})} \quad , \tag{B14}$$

where $\alpha = l_1/(l_1 + l_2)$. This is a kind of simplified averaging process. The final expression for ΔE_{tot} is thus obtained.

The value of K is determined as follows. By using relations

$$\alpha = l_1/(l_1 + l_2) = l_1/2l_{(1)} \quad , \quad l_{(1)} = (C/2\sigma)^{1/2} \quad ,$$

$$n(\alpha) = (2l_{(1)}/aC)\alpha(1 - \alpha)(\sigma b l_{(1)} - f) + \tfrac{3}{4} \quad ,$$

$$n(\tfrac{1}{2}) = 1 \quad , \tag{B15}$$

$$\Delta\epsilon(\alpha) = \Delta\epsilon(\tfrac{1}{2}) = abl_{(1)} \quad ,$$

$$\Delta\sigma(\alpha) = (1/bl_{(1)})\{2f - aC[4l_{(1)}\alpha(1 - \alpha)]^{-1}\} \quad ,$$

Eq. (B14) can be written

$$K = \frac{\int_{\alpha_m}^{\alpha_M} [\alpha(1 - \alpha) + \tfrac{3}{4}]\{(2f/a)(2C\sigma)^{-1/2} - [4\alpha(1 - \alpha)]^{-1}\}\, d\alpha}{(2f/a)(2C\sigma)^{-1/2} - 1} \quad . \tag{B16}$$

The integrand in the above expression is positive when $\alpha_m \leqslant \alpha \leqslant \alpha_M$, and in this range of α hysteresis loss arises. Note that this condition is the same as the condition $\Delta\sigma \geqslant 0$. The α_m and α_M are determined as the two roots of the equation

$$(2f/a)(2C\sigma)^{-1/2} - [4\alpha(1 - \alpha)]^{-1} = 0 \quad . \tag{B17}$$

By using typical experimental values of $\sigma = 10^3$ dyn/cm^2 and $f = 6 \times 10^{-10}$ dyn, one obtains $\alpha_m = 0.17$ and $\alpha_M = 0.83$. Finally, from Eq. (B16) the value $K = 0.39$ is obtained by numerical integration.

APPENDIX C: CALCULATION OF DAMPING CONSTANT

Two kinds of three-phonon process

$$(\omega_1, \vec{q}^{\,1}) + (\omega_2, \vec{q}^{\,2}) \rightarrow (\omega_3, \vec{q}^{\,3}) \quad , \tag{C1}$$

$$(\omega_1, \vec{q}^{\,1}) \rightarrow (\omega_2, \vec{q}^{\,2}) + (\omega_3, \vec{q}^{\,3}) \tag{C2}$$

are considered, where ω_i and $\vec{q}^{\,i}$ are the frequency and the wave vector of the ith phonon. From per-

turbation theory, the transition probability is given as

$$P = (2\pi/\hbar)(H_{if})^2 D_f \ , \tag{C3}$$

where P represents the number of occurrences per second, H_{if} is the matrix element of the perturbing Hamiltonian between the final and initial states, and the density of final state D_f is

$$D_f = (\omega_3)^2 V/2\hbar\pi^2 (c_3)^3 \ . \tag{C4}$$

Here c_3 is the phase velocity of the phonon in state 3, and V is the interaction volume of the process. By using the creation and annihilation operators, the matrix element H_{if} can conveniently be calculated as

$$H_{if} = [(2\hbar)^{3/2} Q q^1 q^2 q^3 (\omega_1\omega_2\omega_3)^{-1/2}](N_1 N_2)^{1/2} \ , \tag{C5}$$

$$H_{if} = [(2\hbar)^{3/2} Q q^1 q^2 q^3 (\omega_1\omega_2\omega_3)^{-1/2}][N_1(N_2+1)]^{1/2} \ . \tag{C6}$$

Equations (C5) and (C6) correspond to the processes represented in Eqs. (C1) and (C2), respectively. Here N_i is the number of phonons in the ith state, q^i is the magnitude of the vector $\vec{q}^{\,i}$, and the factor Q represents the strength of the interactions between phonons. In the continuum approximation, after expanding the elastic potential energy density of the material to the cubic terms in strains, Q is expressed as

$$Q = (2!)^{-1} \sum_{efghl} 2c_{efgh}(\hat{p}_g^1 \hat{p}_l^2 \hat{p}_l^3 \hat{q}_h^1 \hat{q}_e^2 \hat{q}_f^3 + \hat{p}_g^2 \hat{p}_l^3 \hat{p}_l^1 \hat{q}_h^2 \hat{q}_e^3 \hat{q}_f^1 + \hat{p}_g^3 \hat{p}_l^1 \hat{p}_l^2 \hat{q}_h^3 \hat{q}_e^1 \hat{q}_f^2)$$
$$+ (3!)^{-1} \sum_{rstuvw} 6C_{rstuvw} \hat{p}_r^1 \hat{p}_t^2 \hat{p}_v^3 \hat{q}_s^1 \hat{q}_u^2 \hat{q}_w^3 \ . \tag{C7}$$

In the above expression, $\hat{q}_j^i$ is the jth component of the wave vector and $\hat{p}_k^i$ is the kth component of the polarization vector for the ith phonon, and c_{efgh} and C_{rstuvw} are the second- and the third-order elastic constants. In this case of long-wavelength limit, the relation $q^i = \omega_i/c_i$ can be used in Eqs. (C5) and (C6), where c_i is the phase velocity of the ith phonon.

For the case of the processes represented by Eq. (25), the frequencies of phonons are $\omega_1 = \omega_0$, $\omega_2 = \Delta\omega$, and $\omega_3 = \omega_0 + \Delta\omega$ in Eq. (C5) and $\omega_1 = \omega_0$, $\omega_2 = \Delta\omega$, and $\omega_3 = \omega_0 - \Delta\omega$ in Eq. (C6). In both cases the approximation $\omega_3 \approx \omega_0$ can be adopted, since $\Delta\omega/\omega_0 = v/c << 1$. Then it can be shown that the difference of the probabilities of two processes is

$$P_2 - P_1 = \left(\frac{\hbar Q^2}{8\pi\rho^3}\right) N_1 \omega_0^4 \Delta\omega (c_1 c_2)^{-2} d_3^{-5} \ . \tag{C8}$$

When the quasilocal phonons are assumed to exist in a cylindrical region or radius r around dislocation line, their number is

$$N_1 = \tfrac{2}{3}\pi r^2 N_v (e^{\hbar\omega_0/k_B T} - 1)^{-1} \tag{C9}$$

per unit length of dislocation. Here N_v is the number of atoms per unit volume, and the factor $\frac{2}{3}$ means that the vibrational modes normal to the dislocation line are taken into account. The damping constant can be obtained by using Eqs. (26), (27), (C8), and (C9). The result is

$$B = \frac{\hbar^2 \omega_0^6 N_v r^2 Q^2}{6\pi\rho^3 c_1^4 c_2^2 c_3^5} \exp\left(-\frac{\hbar\omega_0}{k_B T}\right) \ , \tag{C10}$$

where the condition $\hbar\omega_0/k_B T >> 1$ is adopted. This condition holds in the present case, since $\omega_0 = 12-14$ K and $T = 1.3-2.3$ K.

Finally, the modes of the interacting phonons are considered. From the momentum conservation condition, the three-phonon processes $L + T \rightarrow L$ and $T + T \rightarrow L$ are usually considered to be most frequent (L: longitudinal phonons, T: transverse phonons). However, when the energy uncertainty of the thermal phonons is taken into consideration, other processes, for example $T + T \rightarrow T$, are also possible.[9] This interaction may easily occur in the present case of a collinear process where the frequency of the absorbing or emitting phonon ω_0 is very small. We consider here that the three kinds of interacting phonons are all slow transverse phonons, because such a reaction has the largest contribution to the dislocation damping, as can be seen from Eq. (C10). Then with substitution of $c_1 = c_2 = c_3 = c$ in Eq. (C10), where c is the velocity of the slow transverse sound propagating in the basal plane of the crystal, one finally obtains Eq. (28) in the text. It must be remembered that the velocities of sound propagating in the basal plane are all the same.

[1] J. Wilks, *The Properties of Liquid and Solid Helium* (Clarendon, Oxford, 1967).

[2] R. A. Guyer, in *Solid State Physics*, edited by F. Seitz, D. Turnbull, and H. Ehrenreich (Academic, New York, 1969), Vol. 23, p. 413.

[3] C. M. Varma and N. R. Werthamer, in *The Physics of Liquid and Solid Helium*, edited by K. H. Bennemann and J. B. Ketterson (Wiley, New York, 1976), Part I, p. 503.

[4] H. R. Glyde, in *Rare Gas Solids*, edited by M. L. Klein and J. A. Venables (Academic, New York, 1976), Vol. I, p. 382.

[5] Y. Hiki and F. Tsuruoka, in *Proceedings of the Fourteenth International Conference on Low Temperature Physics*, edited by M. Krusius and M. Vuorio (North-Holland, Amsterdam, 1975), Vol. 1, p. 479.

[6] Y. Hiki and F. Tsuruoka, Phys. Lett. A 56, 484 (1976).

[7]Y. Hiki and F. Tsuruoka, Phys. Lett. A 62, 50 (1977).
[8]Y. Hiki and F. Tsuruoka, in *Proceedings of the Sixth International Conference on Internal Friction and Ultrasonic Attenuation in Solids,* edited by R. R. Hasiguti and N. Mikoshiba (University of Tokyo, Tokyo, 1977), p. 55.
[9]R. Truell, C. Elbaum, and B. B. Chick, *Ultrasonic Methods in Solid State Physics* (Academic, New York, 1969).
[10]K. R. Atkins and R. A. Stasior, Can. J. Phys. 31, 1156 (1953).
[11]E. R. Grilly and R. L. Mills, Ann. Phys. (N.Y.) 8, 1 (1959).
[12]J. P. Franck and R. Wanner, Phys. Rev. Lett. 25, 345 (1970).
[13]R. H. Crepeau, O. Heybey, D. M. Lee, and S. A. Strauss, Phys. Rev. A 3, 1162 (1971).
[14]D. S. Greywall, Phys. Rev. A 3, 2106 (1971).
[15]D. S. Greywall, Phys. Rev. B 16, 5127 (1977).
[16]R. Wanner, Ph.D. thesis (University of Alberta, 1970) (unpublished).
[17]T. Kishimoto and O. Nomoto, J. Phys. Soc. Jpn. 9, 1021 (1954).
[18]A. V. Granato and K. Lücke, J. Appl. Phys. 27, 583 (1956); 27, 789 (1956).
[19]R. M. Stern and A. V. Granato, Acta Metall. 10, 358 (1962).
[20]R. E. Green, Jr. and T. Hinton, Trans. Am. Inst. Min. Eng. 236, 435 (1966).
[21]F. R. N. Nabarro, *Theory of Crystal Dislocations* (Clarendon, Oxford, 1967).
[22]A. Seeger, Philos. Mag. 46, 1194 (1955).
[23]A. Seeger, in *Report on the Conference of Defects in Crystalline Solids, Bristol, 1954* (Physical Society, London, 1955), p. 391.
[24]J. P. Hirth and J. Lothe, *Theory of Dislocations* (McGraw-Hill, New York, 1968).
[25]B. R. Tittmann and H. E. Bömmel, Phys. Rev. 151, 178 (1966).
[26]W. B. Gauster and M. A. Breazeale, Phys. Rev. 168, 655 (1968); J. A. Bains, Jr. and M. A. Breazeale, Phys. Rev. B 13, 3623 (1976).
[27]J. D. Eshelby, Proc. R. Soc. London Sect. A 197, 396 (1949).
[28]G. Leibfried, Z. Phys. 127, 344 (1950).
[29]W. P. Mason, J. Acoust. Soc. Amer. 32, 458 (1960).
[30]A. D. Brailsford, J. Appl. Phys. 43, 1380 (1972).
[31]T. Ninomiya, J. Phys. Soc. Jpn. 36, 399 (1974).
[32]R. E. Peierls, *Quantum Theory of Solids* (Clarendon, Oxford, 1965).
[33]A. C. Holt and J. Ford, J. Appl. Phys. 40, 142 (1969).
[34]Y. Kogure and Y. Hiki, J. Phys. Soc. Jpn. 39, 698 (1975).
[35]T. Ninomiya, Nat. Bur. Stand. (U.S.), Spec. Publ. 317, 315 (1970); references cited therein.
[36]P. Leiderer, P. Berberich, S. Hunklinger, and K. Dransfeld, in *Proceedings of the Thirteenth International Conference on Low Temperature Physics,* edited by K. D. Timmerhaus, W. J. O'Sullivan, and E. F. Hammel (Plenum, New York, 1974), Vol. 2, p. 53.
[37]P. Berberich, P. Leiderer, and S. Hunklinger, J. Low Temp. Phys. 22, 61 (1976).
[38]J. H. Vignos and H. A. Fairbank, Phys. Rev. 147, 185 (1966).
[39]I. D. Calder and J. P. Franck, J. Low Temp. Phys. 30, 579 (1978).
[40]I. Iwasa, K. Araki, and H. Suzuki, J. Phys. Soc. Jpn. 46, 1119 (1979).
[41]E. L. Andronikashvili, I. A. Gachechiladze, and V. A. Melik-Shakhnazarov, J. Low Temp. Phys. 23, 5 (1976).
[42]V. L. Tsymbalenko, Zh. Eksp. Teor. Fiz. 74, 1507 (1978).
[43]S. C. Fain, Jr. and D. Lazarus, Phys. Rev. A 1, 1460 (1970).
[44]L. G. Merkulov, Sov. Phys. Tech. Phys. 1, 59 (1956).
[45]F. J. Webb, K. R. Wilkinson, and J. Wilks, Proc. R. Soc. London Sect. A 214, 546 (1952).
[46]J. S. Dugdale and J. P. Franck, Philos. Trans. R. Soc. London 257, 1 (1964).
[47]R. A.Guyer, Phys. Rev. 148, 789 (1966).
[48]A. É. Meierovich, Sov. Phys. JETP 40, 368 (1974).
[49]A. É. Meierovich, Sov. Phys. JETP 44, 617 (1976).
[50]A. É. Meierovich, Sov. Phys. JETP 42, 676 (1975).
[51]J. P. Franck, Phys. Lett. 11, 208 (1964).
[52]A. V. Granato, Phys. Rev. 111, 740 (1958).
[53]S. H. Castles and E. D. Adams, Phys. Rev. Lett. 30, 1125 (1973).
[54]G. Ahlers, Phys. Lett. 22, 404 (1966).
[55]D. S. Greywall, Phys. Rev. Lett. 37, 105 (1976).
[56]A. Andreev, K. Keshishev, L. Mezhov-Deglin, and A. Shal'nikov, Sov. Phys. JETP Lett. 9, 306 (1969).
[57]H. Suzuki, J. Phys. Soc. Jpn. 35, 1472 (1973); 42, 1865 (1977).
[58]V. L. Tsymbalenko, Sov. Phys. JETP 45, 989 (1977).
[59]D. J. Sanders, H. Kwun, A. Hikata, and C. Elbaum, Phys. Rev. Lett. 39, 815 (1977); 40, 458 (1978).
[60]R. Wanner, I. Iwasa, and S. Wales, Solid State Commun. 18, 853 (1976).
[61]I. Iwasa, K. Araki, and H. Suzuki, in *Proceedings of the Sixth International Conference on Internal Friction and Ultrasonic Attenuation in Solids,* edited by R. R. Hasiguti and N. Mikoshiba (University of Tokyo, Tokyo, 1977), p. 549.
[62]A. F. Andreev, Sov. Phys. JETP 41, 1170 (1976); Sov. Phys. Usp. 19, 137 (1976).
[63]B. V. Petukhov and V. L. Pokrovskii, Sov. Phys. JETP 36, 336 (1973).